THE EFFECTS OF HIGH-FAT DIET INDUCED INSULIN RESISTANCE ON CARDIAC STRUCTURE, FUNCTION, AND LIPID PROFILE

Brinda Sarathy

A Senior Honors Project Presented to the

Honors College

East Carolina University

In Partial Fulfillment of the

Requirements for

Graduation with Honors

by

Brinda Sarathy

Greenville, NC

May, 2020

Approved by:

Dr. Jitka Virag

Department of Physiology, The Brody School of Medicine

ABSTRACT

Intracardiac injection of recombinant EphrinA1-Fc immediately following coronary artery ligation in mice reduces infarct size in both reperfused and non-reperfused myocardium. These protective effects occurred via modulation of the inflammation, autophagic, and apoptotic signal cascades as well as interstitial fibrosis. Given the prevalence of heart disease and poor prognoses in the diabetic population, this project aims to understand the effects of a high-fat diet(HFD) on the heart and cardiac lipid profile and mechanism by with HFD models are associated with poorer outcomes to investigate the potential therapeutic utility of ephrinA1-Fc in the diabetic, ischemic heart. 5-6 wk-old C57BL6J male and female mice were fed a high-fat diet for 12 weeks to induce insulin resistance. Echocardiography was conducted to measure cardiac structure and function. Mice were sacrificed and hearts were either frozen or embedded in paraffin. Glycogen content assays and liquid-chromatography mass spectrometry (LC/MS) were conducted on frozen hearts to assess glycogen content and cardiac lipid profile. Immunohistochemistry and histology staining were conducted on fixed tissue sections to assess inflammation and fibrosis. Male HFD mice experienced a significant reduction in ejection fraction and fractional shortening and a significant increase in systolic and diastolic chamber dimensions, while female HFD mice exhibited decreased LV mass/body weight ratio. Male HFD models exhibited altered structure and inflammation levels, as evidenced by increased inflammation, fibrosis, and hypertrophy/myocyte cross-sectional area, which can reduce cardiac function and remodeling capacity. HFD mice displayed a significant decrease in cardiac glycogen content. A significant increase in LDMPE peak area was observed in HFD mice. Preliminary in vitro studies using H9c2 cells treated with estradiol suggest that time and dose of ephrinA1 may influence estradiol mediated changes in ephrinA1/EphA. From these results, it is possible that EphrinA1-Fc (EA1) could be used to combat the impairment caused by HFD feeding. Further studies are necessary to investigate the cardiac modeling consequences of injecting a therapeutic dose of EphrinA1-Fc at the time of myocardial infarction in HFD models.

INTRODUCTION

Type 2 Diabetes Mellitus (T2DM), caused by a combination of insulin resistance and deficiency, affects 21 million adults across the United States (Bullard et. al, 2016). Consumption of a high-fat diet (HFD) is associated with increased weight gain, fat deposition, hyperglycemia, and insulin resistance, as well as a higher risk of type 2 diabetes mellitus and obesity in humans (McLaughlin et al., 2016). T2DM can reduce life expectancy by as much as 10 years, and the primary cause of death for individuals with T2DM is cardiovascular disease (CVD) (Einarson et al., 2018, Leon & Maddox, 2015). Individuals with T2DM are more likely to suffer a myocardial infarction (MI), which can result in fatal consequences (Leon & Maddox, 2015).

Ischemic heart disease (IHD) is the leading cause of death worldwide, with myocardial infarction presenting as the most common cause of morbidity and mortality (Teringova & Tousek, 2017). One key marker of IHD is apoptosis, a type of programmed cell death, which occurs via activation of specific signaling cascades. High levels of apoptosis are present at the subacute phase of MI and correlate with left ventricle remodeling in response to injury. In cardiomyocytes, apoptosis can be induced by TNF-α (tumor necrosis factor alpha), a proinflammatory cytokine. T2DM is a comorbidity of obesity and ischemic heart disease , making experimental diet-induced models of obesity useful for studying the effects of T2DM and ischemic CVD (Figure 1) (Poncelas et al., 2015).

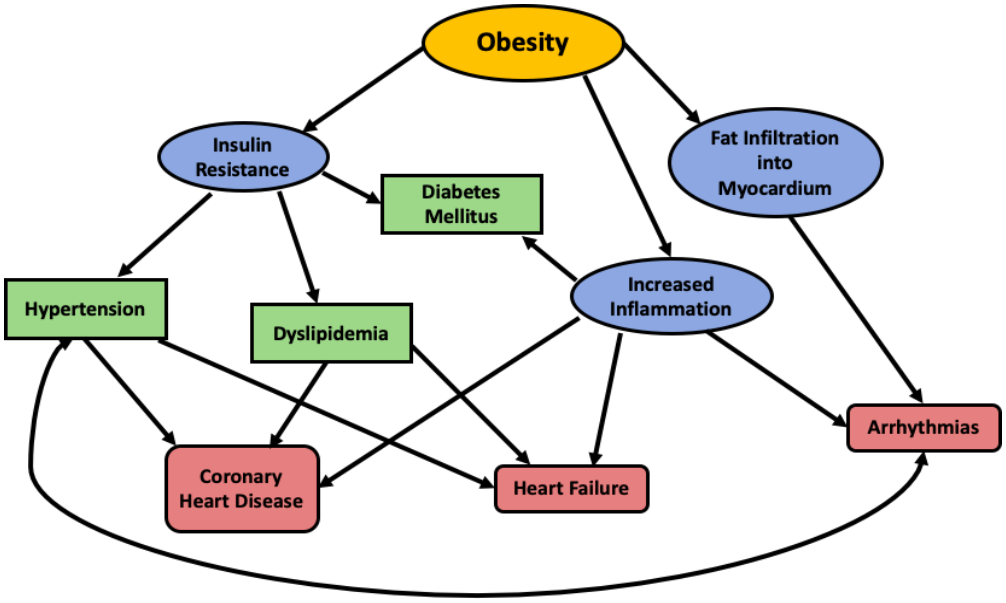

Figure 1: **Obesity Schematic.** Obesity causes a number of health issues, and is most directly related to insulin resistance, myocardium fat infiltration, and increased inflammation. These can cause chronic illnesses include Type 2 Diabetes Mellitus (T2DM), dyslipidemia, and hypertension. Serious and fatal cardiac complications can arise from these illnesses, including coronary heart disease, heart failure, and arrhythmias.

Clinical evidence and experimental studies using high-fat diet animal models to induce obesity and mimic hyperglycemia and insulin resistance have found that consuming a high-fat diet resulted in larger infarct size, cardiac hypertrophy, myocardial glycogen accumulation, and an increased risk of ventricular arrhythmias and death following myocardial infarction (Figure 1) (Lloyd et al., 2012,Varma et al., 2018). Perturbations related to T2DM and inflammation can also adversely affect wound healing capacity, resulting in poor cardiac remodeling post-myocardial infarction (Okonkwo & DiPietro, 2017). The process of cardiac remodeling can cause increased fibrosis and result in further impairment of cardiac function and heart failure (Talman & Ruskoaho, 2016).

Mitochondrial function has been recognized as a key factor in CVD and MI. By manipulating the metabolic profile of cardiomyocytes during ischemia/reperfusion (I/R) injury, it may be possible to mitigate tissue injury.

Eph receptors and their Ephrin ligands are regulators of various cell proliferation, motility, survival, and metabolic signaling pathways. We have discovered that EphrinA1, a membrane-anchored receptor tyrosine kinase ligand that is expressed in healthy cardiomyocytes, is and lost following an ischemic event. In our laboratory, previous studies using an intramyocardial injection of recombinant EphrinA1-Fc (at the time of permanent left anterior descending (LAD) coronary artery ligation was found to relieve the negative effects of cardiac remodeling and substantially reduced infarct size 4 days after permanent occlusion in mice via modulation of the inflammation, autophagic, and apoptotic signal cascades as well as interstitial fibrosis (Dries et al., 2011). We have also recently found that intracardiac administration of recombinant ephrinA1-Fc (EA1)preserves mitochondrial bioenergetics during acute ischemia/reperfusion injury and this correlated with less lipid droplet accumulation indicating reduced lipotoxicity as well as preserved mitochondrial network integrity and cardiomyocyte ultrastructure (Torres et al., 2019). Additionally, we have observed increased pAkt/Akt, which is a known anti-apoptotic signaling mediator in cardioprotection (Dries et al., 2011). The PKB/Akt pathway phosphorylates and regulates the function of many cellular proteins involved in processes that include metabolism, apoptosis, and proliferation (Dries et al., 2011). Akt inhibits transcription factors that promote the expression of cell death genes and enhances transcription of anti-apoptotic genes. Insulin resistance present in T2DM is characterized by decreased pAkt/Akt and, as such, represents a pivotal signaling point for the interruption of apoptosis and adverse metabolic effects by ephrinA1-Fc administration (Dries et al., 2011).

Dyslipidemia, an elevated amount of serum lipids, is associated with T2DM and CVD, and is a result of disrupted lipid metabolism (Leon & Maddox, 2015, Kohno et al., 2018). Preliminary data from the Virag lab has also shown that EphrinA1-Fc decreases lipid droplet accumulation, leading to the hypothesis that intramyocardial injection of EphrinA1-FC at the time of infarction may attenuate lipotoxicity and metabolic dysfunction in HFD models (Dries et al., 2011). Lipidomic profiling, a technique used to evaluate the comprehensive lipid profile in a sample using mass spectrometry, is a powerful tool to explore biomarkers and mechanisms in cardiovascular diseases (Kohno et al., 2018).

The relative risk for CVD morbidity and mortality in adults with diabetes ranges from 1 to 3 in men and from 2 to 5 in women compared to those without DM (Leon & Maddox, 2015). Previous studies have shown that the female sex is associated with a lower risk of cardiac ischemic events and smaller infarct size compared to males (Barba et al. 2017). Moreover, female sex mice fed a standard diet show higher resistance to lipid serum oxidation (Barba et al. 2017). We have previously measured higher baseline levels of endogenous ephrinA1 in female myocardium which may contribute to the observed protection.

Given the prevalence of heart disease and poorer prognoses in the diabetic population, understanding the effects of a high-fat diet on the cardiac lipid profile and examining sex-related differences in HFD models would enable us to determine the mechanism by which HFD models are associated with poorer outcomes and investigate the potential therapeutic utility of ephrinA1-Fc in the diabetic, ischemic heart. Specifically, this project aims to assess the cardiac effects of insulin resistance induced by 12 weeks of 60%kcal high fat diet (HFD) feeding in two groups of mixed-sex mice (one control normal chow diet and one insulin-resistant HFD group) on endogenous ephrinA1 expression, cardiac function via echocardiography, histology/immunohistochemistry staining for morphometric measures, inflammatory cells, and interstitial fibrosis, liquid-chromatography mass spectrometry for cardiac lipid profiling, and glycogen content assays.

METHODS

Animals and Ethical Statement. All animal research protocols were approved by the East Carolina University Institutional Animal Care and Use Committee (IACUC) following the guidelines of the National Institutes of Health for the Care and Use of Laboratory Animals. The Department of Comparative Medicine at The Brody School of Medicine, East Carolina University, maintained animal care.

1) Feeding, blood measures

5-6 week old male and female C57BL6J mice were purchased from the Jackson Laboratory and housed in a temperature-controlled (22 °C) facility with a 12 h light/dark cycle. Mice were randomized to a sham-operated control feeding group (ECU Standard chow) (n= 16) or fed a 60% kcal fat diet (High-Fat Diet - HFD) (n=16). Mice had free access to food and water for 12 weeks, then were weighed and fasted at 18 weeks to assess insulin and blood glucose levels. Mice were anesthetized and euthanized by cervical dislocation. Hearts were harvested and either frozen for glycogen content and liquid-chromatography mass spectrometry (LC/MS) or preserved in a zinc-based fixative, transversely sectioned, and embedded in paraffin. Paraffinized hearts were sectioned at 5 µm and mounted on slides for histology and immunohistochemistry staining.

2) Echocardiography

Mice were conscious and gently restrained in a prone position on a plexiglass board using elastic cord and wire loops on each limb. Using an MX400 22–55 MHz linear-array transducer (Vevo 3100 Imaging System, VisualSonics, Toronto, Canada), standard short- and long-axis views were obtained at the mid-papillary level in both M − and B-mode at >200 frames/second (Dusablon et al. 2017, Lindsey et al., 2018). Echocardiographic images showing the parasternal long-axis view (PSLAX) were used to obtain LS and GLS measurements (Dusablon et al. 2017, Lindsey et al., 2018). Four endocardial points were selected on the echo in a frame between systole and diastole (Dusablon et al. 2017, Lindsey et al., 2018). Analyses were done via Vevo imaging software.

3) Fibrosis and inflammation

To examine fibrosis, picrosirius red/fast green staining was performed using 5-µm sections. Slides were stained with picrosirius red for fibrillar collagen, and the cytoplasm was counterstained with fast green for contrast (Virag et al., 2007). Five images at ×400 were taken in the posteroseptal region. Using Adobe Photoshop software (Adobe Systems, Mountain View, CA), the red collagen fibril pixels were counted and expressed as a percentage of the total number of pixels (total = green + red − white) (Virag et al., 2007).

Immunostaining was performed using 5-µm sections to measure macrophage (pan-leukocyte) density. Tissue sections were deparaffinized in xylene and endogenous peroxidases quenched with 3% H2O2 in methanol (Dries et al., 2011). Slides were rinsed in PBS and incubated with anti-CD45 antibody(PharMingen; 1:2000). The reaction product was visualized with DAB (Vector, SK-4100), counterstained with methyl green, dehydrated in xylene, and slides were coverslipped (Dries et al., 2011). Leukocyte density was measured in three fields per section of two sections of infarcted heart at ×400 (Dries et al., 2011). Results were expressed as the number of cells per 0.1 mm^2.

4) Lipidomics

Hearts were isolated for lipid isolation. Samples were prepared according to Sigma-Aldrich Extraction kit (Catalog#: MAK174). Extracted lipids were identified using an Eskigent 425 microLC/SCIEX 5600 + Triple time-of-

flight mass spectrometer(17). Samples and standards in autosampler vials were placed in a refrigerated holder (8°C). A HALO C18, 2.7 µm, 0.5 × 50 mm microLC column purchased from Eksigent was maintained at 25 °C (Wu et al., 2017). The flow rate was 15 µl/min and 1 µl of sample was injected. Mobile phase A: water with 0.1% formic acid and mobile phase B: acetonitrile with 0.1% formic acid (Wu et al., 2017). Principle component discriminant analysis (PCA-DA) was conducted using LipidView and MarkerView. Pathways were generated via MetaboAnalyst.

5) Glycogen content

Cardiac glycogen levels were assessed by a hexokinase enzymatic reaction (Witczak et al., 2006). Hearts were weighed and a 250 µl aliquot of 2.0 N HCl was added to the sample and then boiled for 2 hours at 95 °C (Witczak et al., 2006). Samples were neutralized by the addition of 250 µl of 2.0 N NaOH, vortexed, and then centrifuged at 13,000g for 30 s. 10µl of 1-M buffer Tris was added to each sample (pH: 7.6) (Witczak et al., 2006). Prepared glucose standards ranging from 0.1094-7mM dissolved in MilliQ ddH2O were added to a 96 well microplate (Witczak et al., 2006). Glycogen levels were assessed using hexokinase reagent (CIMA Scientific, Cat#2820-3, De Soto, TX) (Witczak et al., 2006). Plate was read in a spectrophotometer at 340 nm (Witczak et al., 2006).

6) In vitro studies:

Cell Culture:

For all cell culture experiments the murine cardiomyocyte cell line H9c2 was used in ATCC-formulated Dulbecco's Modified Eagle's Medium (Catalog No. 30 2002) supplemented with 10% fetal bovine serum at 37°C in a humidified incubator containing 5% CO_2. When cells covered 80% of the bottom of the culture container, the cells were treated with trypsin to obtain a single cell suspension, and then seeded into different culture plates for experiments run in duplicate. Plates were pre-treated with a 0.02% gelatin, 0.05% fibronectin solution in dH_2O. Cells were subjected to varying durations (6 hours or 24 hours) and doses of 17β-Estradiol (1 nM, 100 nM, 1 µM) in media.

CAT #	Description
Mm00445804_m1	EphA1 TaqMan primer
Mm00438726_m1	EphA2 TaqMan primer
Mm00580743_m1	EphA3 TaqMan primer
Mm00433056_m1	EphA4 TaqMan primer
Mm00433074_m1	EphA5 TaqMan primer
Mm00433094_m1	EphA6 TaqMan primer
Mm01217450_m1	Epha7 TaqMan primer
Mm00433106_m1	Epha8 TaqMan primer
Mm01212795_m1	EfnA1 TaqMan primer
Mm00433011_m1	EfnA2 TaqMan primer
Mm01212723_g1	EfnA3 TaqMan primer
Mm00433013_m1	EfnA4 TaqMan primer
Mm01237700_m1	EfnA5 TaqMan primer
Mm00433016_m1	EfnB3 TaqMan primer

Figure 2: **RT-PCR Assay ID's.** TaqMan primers utilized for RT-PCR

RNA Extraction and RT-PCR(real-time polymerase chain reaction):

Total RNA was extracted from H9c2 cells. 1 mL of TRIzol reagent (ThermoFisher 15596026) per 10 cm^2 of culture dish was added to each well. Lysate was vortexed, washed with 100 µl chloroform and centrifuged at 12,000 x g at 4°C for 15 mins. 250 µl of isopropanol was added and samples were centrifuged at 12,000 x g at 4°C and chilled overnight at -20°C . Samples were washed twice with 500uL of 80% ethanol, and pellet was dissolved in 20-25 µl of RNA-ase-free dH_2O.

RNA was quantified using Nanodrop at 260 and 280 nm. cDNA was synthesized using RT^2 First Strand Kit (Qiagen 330401). cDNA was diluted 1:1 in DNase-, RNase- and protease-free water (Applichem, Darmstadt, Germany) and 10-100 ng template was used. RT-PCR master mix was made using TaqMan Master Mix (Lot #: 1504094) and listed primers for EphA1-8, EfnA1-5, and EfnB3 RT-PCR were used for running RT-PCR using Thermal Cycler Px2 (Thermo).

7) Statistics

All graphs were generated, and results were analyzed using GraphPad Prism 7.0a or Excel. Significant differences among paired treatment groups were determined using Student's t-test with a significance level of $p < 0.05$.

RESULTS

HFD mice had higher body weights, and male mice weighed more on average than female mice. Female HFD mice did not experience significant change in HOMA-IR values, though male mice exhibited a significant increase in HOMA-IR values after HFD feeding. Female HFD mice exhibited slow return to lowered blood glucose during GTT.

	Control Male (n=16)	Control Female (n=16)	HFD Male (n=16)	HFD Female (n=16)
Body weight (g):	32.3	22.5	43.4	29.4
~14 Fasted Blood Glucose (mM):	4.9 +/- 0.2	4.3 +/- 0.2	5.5 +/- 0.3	5.3 +/- 0.2
~14 Fasted Blood insulin (pM):	204.4 +/- 51.9	230.3 +/- 71.7	356.7 +/- 73.2	193 +/- 35.3
HOMA-IR (mU/L x mM):	5.8 +/- 1.4	5.6 +/- 1.6	13.9 +/- 3.5	6.2 +/- 1.1

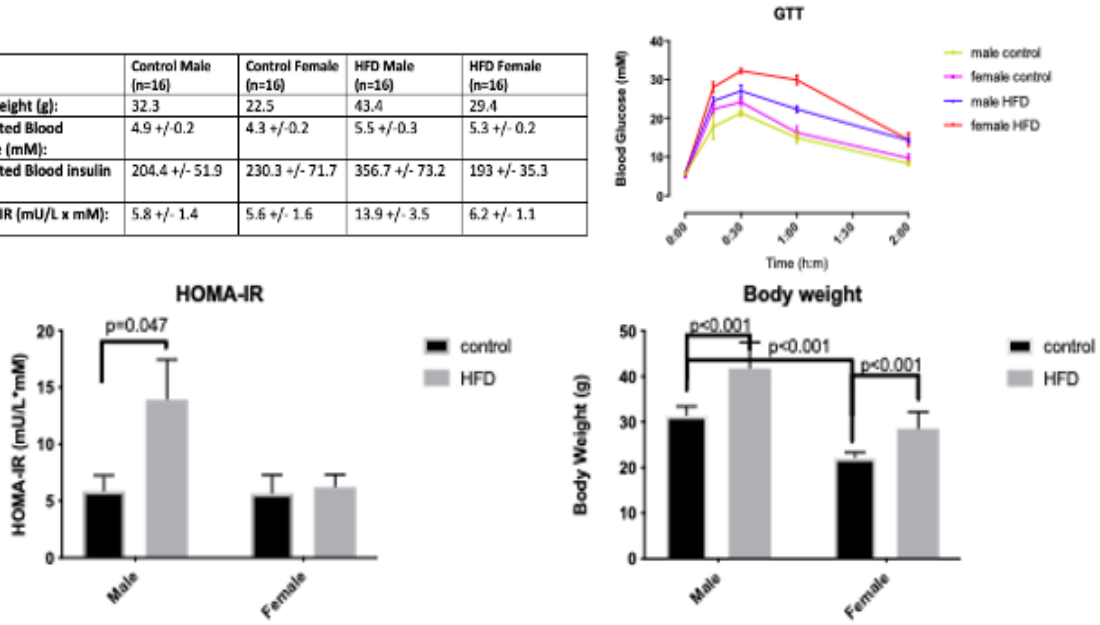

Figure 3: **Blood measures and measures of insulin resistance.** GTT: glucose tolerance test; HOMA-IR: homeostasis assessment model of insulin resistance. Two-way ANOVA tests were performed in HOMA-IR and body weight variables, and data are expressed as means ± SEM (N=16 mice/group).

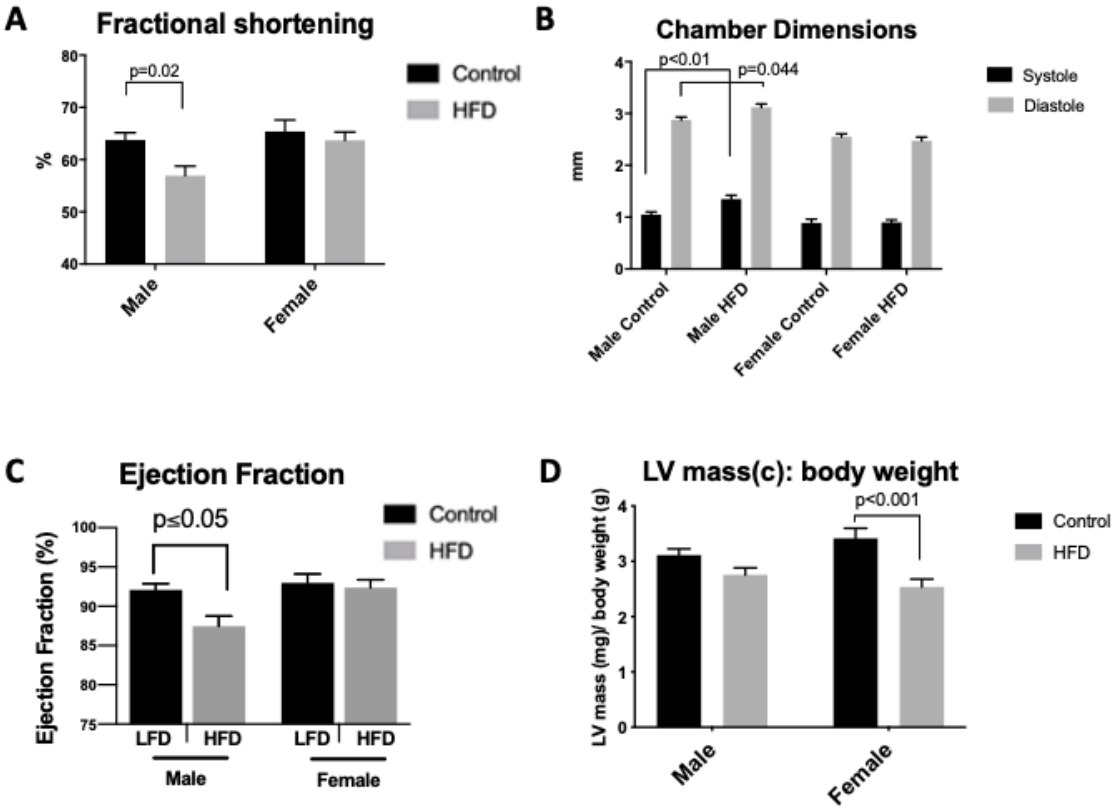

Figure 4. **Echocardiographic analysis**. Echocardiographic measures of LV function and structure: ejection fraction (EF %), fractional shortening (FS %), chamber dimensions (mm) and LV mass/body weight (mg/g). Male HFD mice experienced a significant reduction in ejection fraction and fractional shortening and a significant increase in systolic and diastolic chamber dimensions. Female HFD mice exhibited decreased LV mass/body weight ratio. Data are expressed as means ± SEM. N = 4 mice/group.

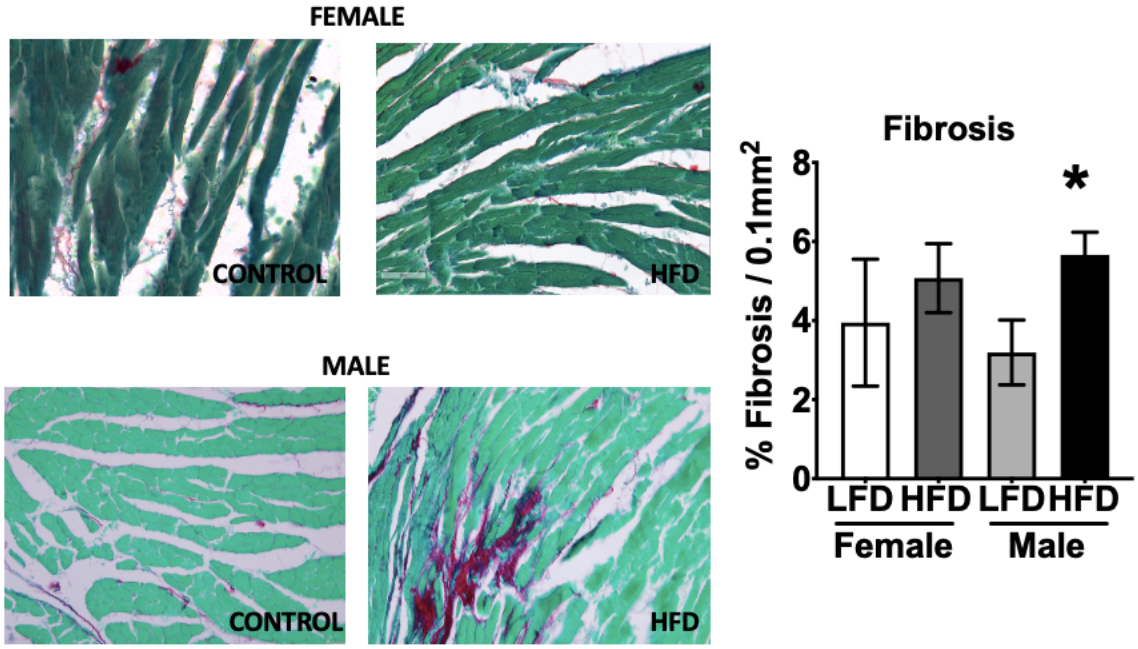

Figure 5. **Interstitial Fibrosis.** Representative picrosirius red/fast green staining of female (above) and male (below) control/HFD remote myocardium (40x) (left). Histological measures of fibrosis (%fibrosis/0.1 mm^2) (right). Male HFD mice exhibited increased levels of fibrosis. Data are expressed as means ± SD. N = 9–12 mice/group. ($p < 0.05$*)

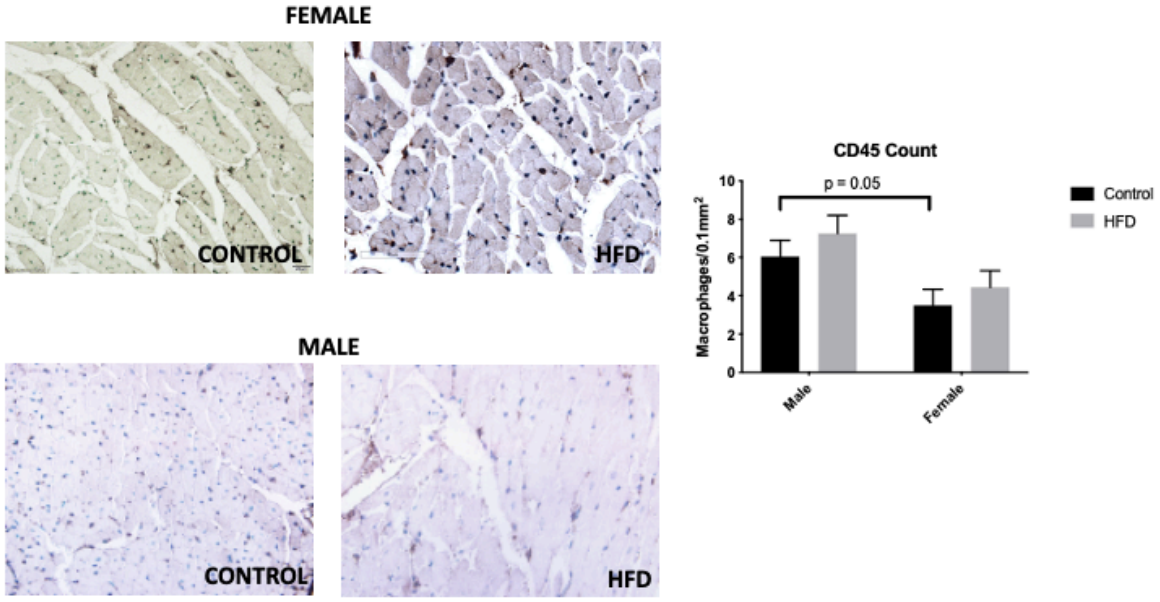

Figures 6: **Macrophage Density**. Representative immunohistochemistry stain of control/HFD female (above) and male (below) remote myocardium (40x) (left). Immunological measures of inflammation (macrophages/0.1 mm^2). N = 9–12 mice/group (right). Data are expressed as means ± SD. N = 4 mice/group.

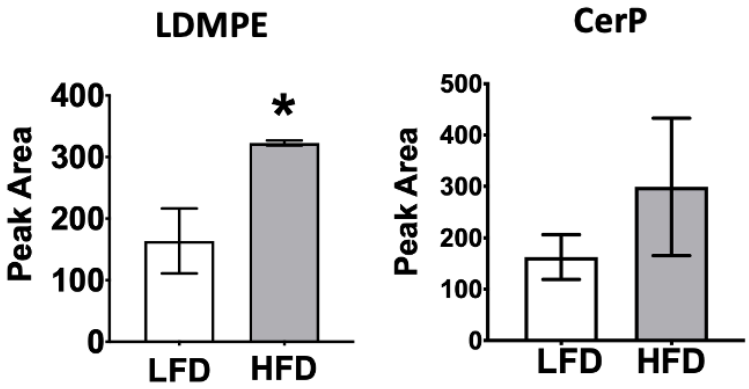

Figure 7: **Lipidomic Analysis**. PCA-DA LC/MS peak area analysis (peak area). Data are expressed as means ± SEM. N = 2-3 mice/group. Significant increase in LDMPE (lysodimethylphosphatidylethanolamine, a type of phophosphoethanolamine and marker of CVD) peak area was observed in HFD mice. Significant change was not observed in CerP peak area (ceramide-phosphate, which blocks insulin signaling and promotes adipose inflammation) (Fang et al., 2019) ($p < 0.05$*)

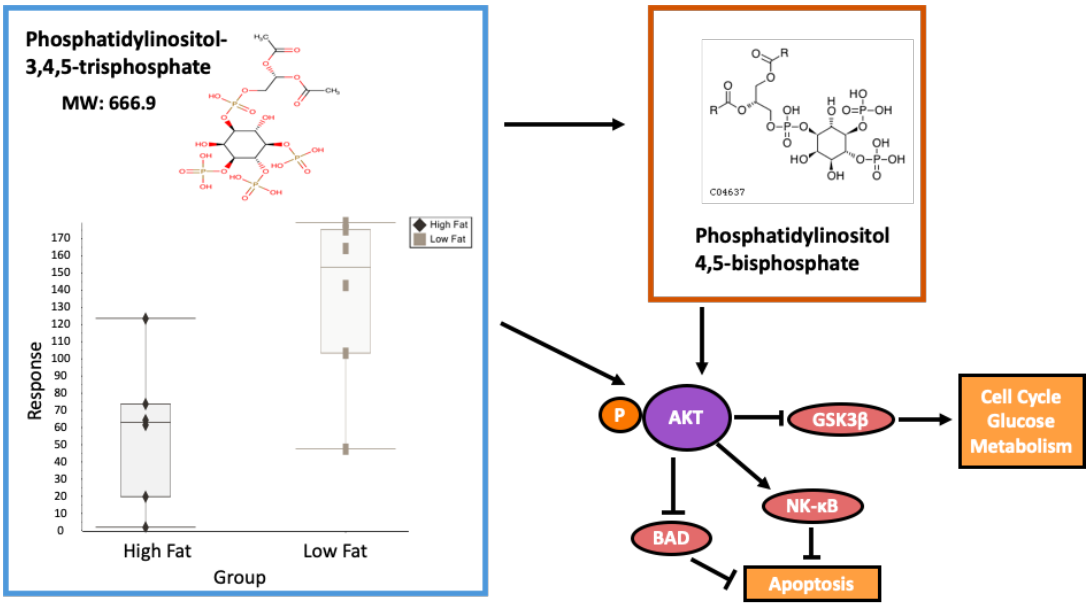

Figure 8: **Phosphatidylinositol pathway diagram**. Increased levels of phosphatidylinositol 3,4,5-triphosphate were observed in LFD mice. Phosphatidylinositol 3,4,5-triphosphate and Phosphatidylinositol 4,5-bisphosphate regulates pAKT signaling. pAKT regulates the function of many cellular proteins and signaling molecules (GSK3$\boldsymbol{\beta}$, NK-κB, and BAD) involved in processes that include metabolism, apoptosis, and the cell cycle.

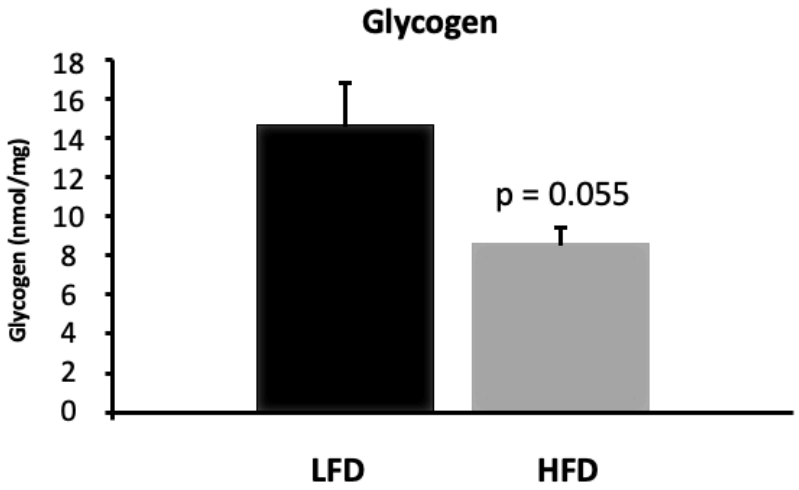

Figure 9: **Glycogen content**. Cardiac glycogen content assay (nmol/mg). Approaching significant decrease in cardiac glycogen content was observed in HFD mice. Data are expressed as means ± SEM. N = 5-6 mice/group.

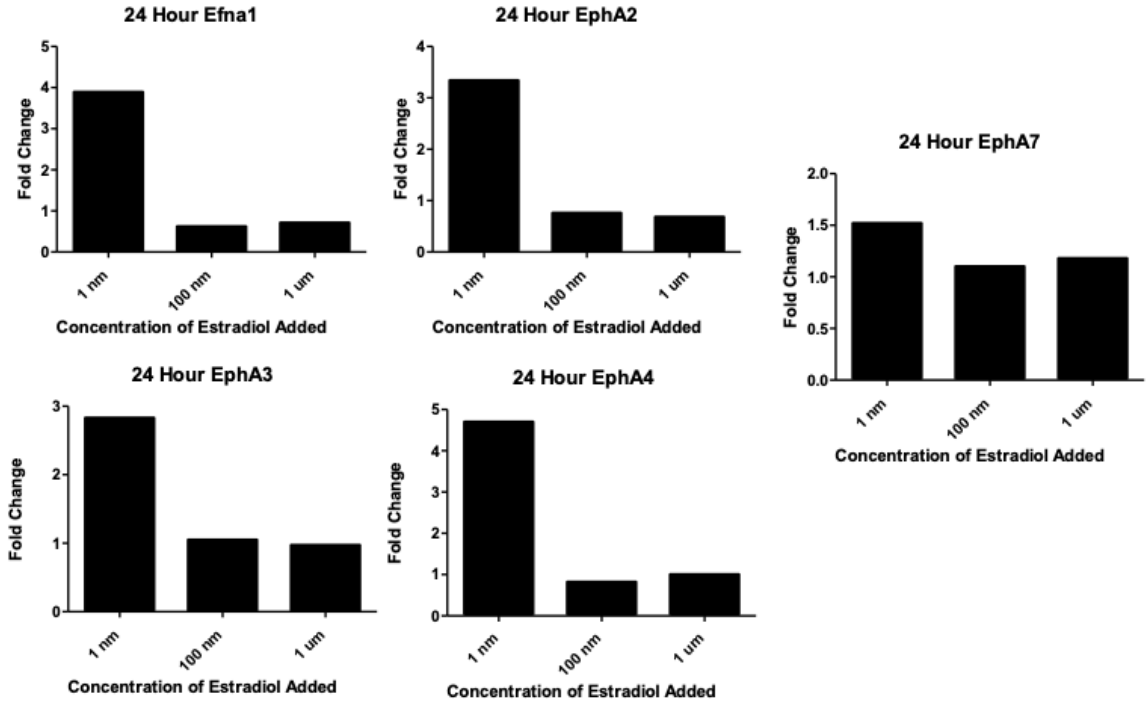

Figure 10: **17β-Estradiol and EphrinA/EphA-Rs.** Preliminary in vitro studies show increases of 3-4x in Efna1, EphA2, EphA3, EphA4, and 1.5x in EphA7 expression during a 24 period of estradiol administration at a 1nm dose. Further testing is necessary to understand the potential for ephrinA1-Fc to synergize with 17β-estradiol to influence the degree of cardioprotection. Data are expressed as relative to control.

DISCUSSION

HFD feeding in mice significantly reduces cardiac function and negatively impacts cardiac structure in male mice, which was seen via echocardiographic imaging. Echocardiographic imaging is a noninvasive means to assess cardiac physiology and heart function in rodent models of heart disease (Lindsey et al., 2018). We determined via echocardiography that male HFD mice experienced a significant reduction in ejection fraction (89% ± 1.059, p = 0.05), and fractional shortening (64.53% ± 1.741, p = 0.02), two measures of cardiac function (FS indicates the percentage change in LV chamber size, whereas EF indicates the percentage change in LV volumes and is an index of LV function (Figure 4) (Lindsey et al., 2018). HFD male mice also exhibited a significant increase in systolic (1.35mm ± 0.26, p <0.01) and diastolic (3.12mm ± 0.23, p=0.044) chamber dimensions (Figure 4). Our previous males-only study also exhibited an increase in cross-sectional myocyte area in HFD mice (285.8 μm^2 ±10.0, p = 0.001) compared to control mice (205.5 μm^2 ± 3.2, p = 0.001). Taken together these results indicate that HFD causes left ventricular hypertrophy.

Male HFD models exhibited altered structure and inflammation levels, as evident by histological and immunological staining. These staining techniques measure fibrosis and inflammation within the heart. Fibrosis is a well-recognized cause of cardiac morbidity and mortality and insulin-resistant models can indicate diabetic hypertrophic cardiomyopathy (Hinderer & Schenke-Layland, 2019). Our results show that male HFD mice displayed increased levels of fibrosis (5.66%/mm^2 ± 0.55, p < 0.05), indicating impaired extracellular matrix (ECM) remodeling, composition, and quality, as well as impaired heart muscle function (Figure 5) (Hinderer & Schenke-Layland, 2019). During periods of cardiac damage and repair, the innate immune system is activated and can trigger an inflammatory response, which can be measured by immunohistochemistry staining for leukocytes (Prabhu & Frangogiannis, 2016). Previously, our results in a males-only study have exhibited increased macrophage density. Our results show that male control mice exhibited increased macrophage density (6.04 macrophages/0.1 mm^2 ± 0.80) compared to female mice, indicative of raised inflammation levels that may translate to impaired reparative response and remodeling post-MI (Figure 6) (Prabhu & Frangogiannis, 2016). This overactive and prolonged inflammatory responses may cause further death of viable cardiomyocytes and extend fibrosis, resulting in an increased predisposition to injury (Frangogiannis, 2015).

Lipidomic profiling allows for the exploration of biomarkers and mechanisms in cardiovascular diseases (Kohno et al. 2018). Triacylglycerides show the most consistent association with cardiovascular disease, along with phosphatidylcholine and phosphatidylethanolamine (Stegemann et al. 2014). Consistent with other data, our results show HFD mice display a significant association with lysodimethylphosphatidylethanolamine (LDMPE) (319.9 ± 5.8, p < 0.05), a type of phosphatidylethanolamine (Figure 7). Our results display a nonsignificant increase of ceramide-phosphate (CerP), which blocks insulin signaling and promotes adipose inflammation (Figure 7)(Fang et al., 2019). Our results also show possible upregulation in the phosphatidylinositol pathway in LFD mice. Activation of this pathway results in upregulated pAkt/Akt, resulting in downregulated cellular functions, including cell survival, proliferation, and cell metabolism (Figure 8) (Mann & Jain, 2015). Further studies are necessary to examine and confirm the differences in lipid metabolism to further understand the mechanisms of dyslipidemia in CVD and HFD models.

During a period of ischemia, coronary blood flow to the heart is reduced and both myocardium oxygen supply and energy substrate supply decrease (Lopaschuk, 2018). This results in reduced mitochondrial oxidative phosphorylation, ATP production, and glucose supply to the heart (Lopaschuk, 2018). To maintain the myocardial glucose supply for glycolysis, glucose is mobilized from endogenous glycogen stores (Lopaschuk, 2018). Consequently, glycogen content can be used as a marker of cardiac pathology (Varma et al. 2018). Excess cardiac glycogen has previously been observed in rats with type 1 diabetes HFD mice and correlated with diastolic dysfunction (Varma et al. 2018). Our results contrast with this; HFD mice displayed a significant

decrease in cardiac glycogen content (8.6nmol/mg ± 0.55, p = 0.055) (Figure 9). Further investigation into glycogen content in the diabetic heart is warranted to further investigate the role of glycophagy in HFD models.

While one third of female deaths are due to ischemic heart disease and stroke and the risk of developing CVD is much greater among women with diabetes than men, the average age of onset for first myocardial infarction is about 10 years later for women compared to men (Humphries et al. 2017). Women with IHD often have better prognoses than men, though this effect is lost in postmenopausal women, suggesting that female sex hormones may play a role in cardioprotection (Humphries et al. 2017). It has been hypothesized that estrogen receptors mediate lipid metabolism via signaling in the liver and increasing LDL cholesterol (Palmisano, 2018). Additionally, a reduction in H_2O_2 production has been observed in female sex, suggesting two different mechanisms of action resulting in a metabolic and oxidative background less susceptible to ischemic damage (Barba et al., 2017). In our study, female HFD mice exhibited fewer impairments as a consequence of HFD, suggesting that gender differences may be involved in providing cardioprotection in HFD models. Specifically, female HFD mice exhibited decreased LV mass/body weight ratio (2.54mg/g ± 0.11, p< 0.001) and no significant change in fibrosis and inflammation. One possible explanation may be the upregulation of the Akt signaling pathways in the presence of 17β-estradiol, thus preventing apoptosis and metabolic dysfunction (Angeloni et al., 2017). Further investigation exposing cardiomyocytes to 17β-estradiol in the presence or absence or ephrinA1-Fc will be helpful to further understand the potential for ephrinA1-Fc to synergize with 17β-estradiol to influence the degree of cardioprotection in female HFD models. We have performed preliminary in vitro studies via RT-PCR demonstrating an interaction between ephrinA1-Fc and 17β-estradiol in modulation of ephrinA/EphA-Rs over a 24-hour period (Figure 10). This interaction may translate to protein expression and downstream signaling. Additional investigation is underway to determine whether these changes are involved in mediating cardioprotection and if they are affected by insulin-resistance.

It is possible that EphrinA1-Fc (EA1) could be used to combat the impairment caused by HFD feeding. Our lab has previous observed that ephrinA1-Fc upregulates the pAkt/Akt pathway, suggesting that ephrinA1-Fc is viable way to counter the decreased pAkt/Akt indicative of insulin resistance. This study has displayed increased fibrosis and glycogen in HFD mice while indicating possible upregulation of the pAkt/Akt pathway in LFD mice, indicating metabolic dysfunction in HFD may be regulated by ephrinA1-Fc. In vitro studies investigating palmitate-induced insulin-resistance in HL-1 and H9C2 cells are necessary and underway to investigate changes in endogenous ephrinA1, pAkt/Akt expression, and metabolomics and further understand the potential of ephrinA1-Fc to attenuate or reverse pAkt/Akt signaling in insulin-resistant models and thereby the susceptibility of the T2DM heart to ischemic disease.

ACKNOWLEDGEMENTS

I would like to thank Dr. Jitka Virag, Uma Sharma, Luke Weyrauch, Samuel Vance, Smrithi Valsaraj, K'Shylah Whitehurst, and Omar Sharaf for facilitating this project, along with the Department of Physiology and the Department of Comparative Medicine at the Brody School of Medicine. Thanks to Dr. Carol Witczak for providing the mice (supported by NIH R01 DK103562), and Ms. Joani Zary for assistance. Funding provided by Summer Biomedical Research Program (SBRP), ECU Undergraduate Research and Creativity Award (URCA) (provided by Division of Research, Economic Development and Engagement at ECU) and NIH-1R15HL124483-0181.

REFERENCES

Angeloni, C., Teti, G., Barbalace, M. C., Malaguti, M., Falconi, M., & Hrelia, S. (2017). 17β-Estradiol enhances sulforaphane cardioprotection against oxidative stress. *The Journal of Nutritional Biochemistry*, *42*, 26–36. doi: 10.1016/j.jnutbio.2016.12.017

Barba, I., Miró-Casas, E., Torrecilla, J. L., Pladevall, E., Tejedor, S., Sebastián-Pérez, R., … García-Dorado, D. (2017). High-fat diet induces metabolic changes and reduces oxidative stress in female mouse hearts. *The Journal of Nutritional Biochemistry*, *40*, 187–193. doi: 10.1016/j.jnutbio.2016.11.004

Bullard, K. M., Cowie, C. C., Lessem, S. E., Saydah, S. H., Menke, A., Geiss, L. S., … Imperatore, G. (2018). Prevalence of Diagnosed Diabetes in Adults by Diabetes Type — United States, 2016. *MMWR. Morbidity and Mortality Weekly Report*, *67*(12), 359–361. doi: 10.15585/mmwr.mm6712a2

Dries, J. L., Kent, S. D., & Virag, J. A. (2011). Intramyocardial administration of chimeric ephrinA1-Fc promotes tissue salvage following myocardial infarction in mice. *The Journal of physiology*, *589*(Pt 7), 1725–1740. https://doi.org/10.1113/jphysiol.2010.202366

Dusablon, A., Parks, J., Whitehurst, K. S., Estes, H., Chase, R., Vlahos, E., … Virag, J. (2017). EphrinA1-Fc attenuates myocardial ischemia/reperfusion injury in mice. *Plos One*, *12*(12). doi: 10.1371/journal.pone.0189307

Einarson, T. R., Acs, A., Ludwig, C., & Panton, U. H. (2018). Prevalence of cardiovascular disease in type 2 diabetes: a systematic literature review of scientific evidence from across the world in 2007-2017. *Cardiovascular diabetology*, *17*(1), 83. https://doi.org/10.1186/s12933-018-0728-6

Fang, Z., Pyne, S., & Pyne, N. J. (2019). Ceramide and sphingosine 1-phosphate in adipose dysfunction. *Progress in Lipid Research*, *74*, 145–159. doi: 10.1016/j.plipres.2019.04.001

Frangogiannis N. G. (2015). Inflammation in cardiac injury, repair and regeneration. *Current opinion in cardiology*, *30*(3), 240–245. https://doi.org/10.1097/HCO.0000000000000158

Hinderer, S., & Schenke-Layland, K. (2019). Cardiac fibrosis – A short review of causes and therapeutic strategies. *Advanced Drug Delivery Reviews*, *146*, 77–82. doi: 10.1016/j.addr.2019.05.011

Humphries, K. H., Izadnegahdar, M., Sedlak, T., Saw, J., Johnston, N., Schenck-Gustafsson, K., Shah, R. U., Regitz-Zagrosek, V., Grewal, J., Vaccarino, V., Wei, J., & Bairey Merz, C. N. (2017). Sex differences in cardiovascular disease - Impact on care and outcomes. *Frontiers in neuroendocrinology*, *46*, 46–70. https://doi.org/10.1016/j.yfrne.2017.04.001

Kohno, S., Keenan, A. L., Ntambi, J. M., & Miyazaki, M. (2018). Lipidomic insight into cardiovascular diseases. *Biochemical and Biophysical Research Communications*, *504*(3), 590–595. doi: 10.1016/j.bbrc.2018.04.106

Leon, B. M., & Maddox, T. M. (2015). Diabetes and cardiovascular disease: Epidemiology, biological mechanisms, treatment recommendations and future research. World journal of diabetes, 6(13), 1246–1258. https://doi.org/10.4239/wjd.v6.i13.1246

Lindsey, M. L., Kassiri, Z., Virag, J. A. I., Brás, L. E. D. C., & Scherrer-Crosbie, M. (2018). Guidelines for measuring cardiac physiology in mice. *American Journal of Physiology-Heart and Circulatory Physiology*, *314*(4). doi: 10.1152/ajpheart.00339.2017

Lloyd, S. G., Liu, J., & Wang, P. (2012). Impact Of High-Fat, Low-Carbohydrate Diet On Myocardial Ischemia / Infarction: An In Vivo Study. *Journal of the American College of Cardiology*, *59*(13). doi: 10.1016/s0735-1097(12)60542-7

Lopaschuk, G. D. (2018). Cardiac energy metabolism in mild and severe ischemia. *Heart and Metabolism*, (75), 33–36. doi: 10.31887/hm.2018.75/lopaschuk

Manna, P., & Jain, S. K. (2015). Phosphatidylinositol-3,4,5-triphosphate and cellular signaling: implications for obesity and diabetes. *Cellular physiology and biochemistry : international journal of experimental*

cellular physiology, biochemistry, and pharmacology, *35*(4), 1253–1275. https://doi.org/10.1159/000373949

McLaughlin, T., Craig, C., Liu, L. F., Perelman, D., Allister, C., Spielman, D., & Cushman, S. W. (2016). Adipose Cell Size and Regional Fat Deposition as Predictors of Metabolic Response to Overfeeding in Insulin-Resistant and Insulin-Sensitive Humans. *Diabetes*, *65*(5), 1245–1254. https://doi.org/10.2337/db15-1213

Okonkwo, U. A., & DiPietro, L. A. (2017). Impaired Wound Repair and Delayed Angiogenesis. *International Journal of Molecular Sciences*, *18*(7). doi: 10.1007/springerreference_168445

Palmisano, B. T., Zhu, L., Eckel, R. H., & Stafford, J. M. (2018). Sex differences in lipid and lipoprotein metabolism. *Molecular Metabolism*, *15*, 45–55. doi: 10.1016/j.molmet.2018.05.008

Poncelas, M., Inserte, J., Vilardosa, Ú., Rodriguez-Sinovas, A., Bañeras, J., Simó, R., & Garcia-Dorado, D. (2015). Obesity induced by high fat diet attenuates postinfarct myocardial remodeling and dysfunction in adult B6D2F1 mice. *Journal of Molecular and Cellular Cardiology*, *84*, 154–161. doi: 10.1016/j.yjmcc.2015.04.023

Prabhu, S. D., & Frangogiannis, N. G. (2016). The Biological Basis for Cardiac Repair After Myocardial Infarction. *Circulation Research*, *119*(1), 91–112. doi: 10.1161/circresaha.116.303577

Stegemann, C., Pechlaner, R., & Willeit, P. (2014). Lipidomics Profiling and Risk of Cardiovascular Disease in the Prospective Population-Based Bruneck Study. *Journal of Vascular Surgery*, *60*(2), 532. doi: 10.1016/j.jvs.2014.06.095

Talman, V., & Ruskoaho, H. (2016). Cardiac fibrosis in myocardial infarction-from repair and remodeling to regeneration. *Cell and tissue research*, *365*(3), 563–581. https://doi.org/10.1007/s00441-016-2431-9

Teringova, E., Tousek, P. Apoptosis in ischemic heart disease. *J Transl Med* **15,** 87 (2017). https://doi.org/10.1186/s12967-017-1191-y

Torres, M. J., Mclaughlin, K. L., Renegar, R. H., Valsaraj, S., Whitehurst, K. S., Sharaf, O. M., … Virag, J. A. (2019). Intracardiac administration of ephrinA1-Fc preserves mitochondrial bioenergetics during acute ischemia/reperfusion injury. *Life Sciences*, *239*, 117053. doi: 10.1016/j.lfs.2019.117053

Varma, U., Curl, C., Janssens, J., Mellor, K., & Delbridge, L. (2018). Diabetes-induced diastolic dysfunction is associated with myocardial glycogen accumulation and disrupted autophagy signalling. *Journal of Molecular and Cellular Cardiology*, *120*, 26. doi: 10.1016/j.yjmcc.2018.05.083

Virag, J. A., Rolle, M. L., Reece, J., Hardouin, S., Feigl, E. O., & Murry, C. E. (2007). Fibroblast growth factor-2 regulates myocardial infarct repair: effects on cell proliferation, scar contraction, and ventricular function. *The American Journal of Pathology*, *171*(5), 1431–1440. https://doi.org/10.2353/ajpath.2007.070003

Witczak, C., Hirshman, M., Jessen, N., Fujii, N., Seifert, M., Brandauer, J., … Goodyear, L. (2006). JNK1 deficiency does not enhance muscle glucose metabolism in lean mice. *Biochemical and Biophysical Research Communications*, *350*(4), 1063–1068. doi: 10.1016/j.bbrc.2006.09.158

Wu, X.-J., Williams, M. J., Patel, P. R., Kew, K. A., & Zhu, Y. (2019). Subfertility and reduced progestin synthesis in Pgrmc2 knockout zebrafish. *General and Comparative Endocrinology*, *282*, 113218. doi: 10.1016/j.ygcen.2019.113218